Oil & Gas Science and Technology – Rev. IFP, Vol. 55 (2000), No. 6, pp. 599-609

Mechanical Behaviour of a Porous Chalk and Water/Chalk Interaction

Part II: Numerical Modelling

S. Homand[1] and J.F. Shao[1]*

1 USTL-EUDIL, Laboratory of Mechanics of Lille, URA 1441, Cité scientifique, 59655 Villeneuve-d'Ascq - France
e-mail: Jian-Fu.Shao@eudil.fr
* Author to whom correspondence should be addressed

Résumé — Comportement mécanique d'une craie poreuse et effets de l'interaction eau/craie, 2e partie : Modélisation numérique* — Cet article est le second volet d'une étude complète du comportement mécanique d'une craie poreuse et des effets du fluide saturant sur celui-ci. Il fait suite à une étude expérimentale sur de la craie poreuse.

Un modèle élastoplastique à deux surfaces de charge y est présenté pour décrire le comportement d'une telle craie. Les déformations plastiques induites par l'injection d'eau, observées expérimentalement, sont modélisées en utilisant un potentiel plastique supplémentaire. Ce potentiel est établi à partir du saut de comportement de la craie lié au fluide saturant. L'utilisation de ce modèle fournit de bonnes simulations des essais présentés dans le premier volet de notre étude.

Mots-clés : comportement mécanique, plasticité, craie, effets de l'eau, modélisation.

Abstract* — *Mechanical Behaviour of a Porous Chalk and Water/Chalk Interaction, Part II: Numerical Modelling — *This paper is the second part of a general work on the mechanical behaviour of a porous chalk and the effect of saturating fluid.*

It presents the development of an elastoplastic model with two yield surfaces to describe the chalk behaviour. The water induced plastic deformation observed experimentally is described by using an additional plastic potential, based on the behaviour jump between two material states of chalk saturated with two different fluids. A good correlation is obtained between numerical simulations and experimental data obtained in the experimental study presented in the first part.

Keywords: mechanical behaviour, plasticity, chalk, water effects, modelling.

---

* La première partie de cet article est publiée dans ce même numéro de *Oil & Gas Science and Technology – Revue de l'IFP*, p. 591-598.

Part I of this paper is published in this issue of Oil & Gas Science and Technology – Revue de l'IFP, *p. 591-598.*

INTRODUCTION

Some valuable theoretical and numerical developments have been formulated for the description of water induced plastic deformation.

Piau and Maury (1994, 1995) and Piau *et al.* (1998) proposed a conceptual model by introducing an additional stress increment which is seen as responsible to the plastic deformation induced by water injection. This model provides a simple conceptual framework. However, the physical meaning of the additional stress and the theoretical background of the formulation remain confuse. Papamichos *et al.* (1997) extended the concepts of unsaturated soils to develop an elastoplastic model. However, in the case of chalk, the validity of suction concept is questionable. Furthermore, continuous variations of chalk properties as functions of water saturation are not clearly shown by experimental data.

On the basis of test data by Schroeder, the authors (Homand *et al.*, 1998) noticed that there is a critical value of water saturation at which a sudden transition from "oil-like" behaviour to "water-like" behaviour takes place. Then a preliminary version of an elastoplastic model has been proposed by introducing the mechanism of yield surface jump when chalk is flooded by water. A similar approach has been used by Piau *et al.* (1998) in Cam-Clay model. However, the validity of the model was not tested against laboratory tests even for basic loading conditions. Furthermore, Schroeder (1995) performed hydrostatic tests on samples saturated with fluids with different viscosity and he has concluded that there is no clear correlation between chalk behaviour and fluid viscosity.

However, two groups of behaviour can clearly be identified when the chalk is saturated by "water-like" fluid and "oil-like" fluid. Therefore, a viscoplastic modelling is not suitable for the description of chalk/water interaction. Nevertheless, chalk usually exhibits time-dependent plastic deformation (Shao *et al.*, 1995) which could be enhanced by the water flooding. But this feature is not investigated in this work.

The purpose of this paper is to develop a new constitutive model for the description of basic mechanical properties of chalk and water induced deformation. The preliminary version of the elastoplastic model proposed by the authors (Homand *et al.*, 1998) is completed and improved. The parameters have been determined from test data presented in the paper concerning the experimental results (Homand and Shao, 2000). A new way is proposed to describe additional plastic deformation induced by water injection.

Comparisons between numerical simulations and experimental data have been done, both for conventional triaxial tests, lateral extension tests, proportional loading tests and specific water injection tests.

PRESENTATION OF THE ELASTOPLASTIC MODEL

Background

The experimental results suggest that the chalk behaviour can be modelled in terms of elastoplastic model with two plastic deformation mechanisms (Halleux *et al.*, 1990; Shao and Henry, 1991; Monjoie *et al.*, 1995; Homand and Shao, 2000). Drucker *et al.* (1957) were the first to introduce a spherical end-cap to the Drucker-Prager model in order to control the plastic volumetric change of soil. Within the framework of small strain elastoplasticity, it is assumed that the total strain increment $d\varepsilon_{ij}$ is obtained from the superposition of an elastic and a plastic parts, $d\varepsilon^e_{ij}$ and $d\varepsilon^p_{ij}$, respectively. The plastic part is then divided into plastic collapse and plastic deviatoric parts, $d\varepsilon^c_{ij}$ and $d\varepsilon^d_{ij}$, respectively:

$$d\varepsilon_{ij} = d\varepsilon^e_{ij} + d\varepsilon^p_{ij} \quad \text{and:} \quad d\varepsilon^p_{ij} = d\varepsilon^c_{ij} + d\varepsilon^d_{ij} \tag{1}$$

The elastic strains $d\varepsilon^e_{ij}$ due to an applied stress increment $d\sigma_{ij}$ are obtained from an elastic stress-strain relation of the form:

$$d\varepsilon^e_{ij} = \frac{1+\nu_0}{E_0}\, d\sigma_{ij} - \frac{\nu_0}{E_0}\, \mathrm{tr}(d\bar{\sigma})\delta_{ij} \tag{2}$$

where E_0 and ν_0 are the elastic parameters, respectively the Young modulus and the Poisson's ratio in drained conditions.

Presentation of the Elastoplastic Model

Pore Collapse Mechanism

From the experimental data (Homand and Shao, 2000), the plastic yield function for the pore collapse mechanism is expressed by:

$$f_c = h^2 q^2 + p^2 - k^2 = 0 \tag{3}$$

with:

$$p = \frac{\sigma_{ii}}{3} \tag{4}$$

$$q = \sqrt{3J_2} = \sqrt{\frac{3}{2} s_{ij} s_{ij}} \quad \text{with:} \quad s_{ij} = \sigma_{ij} - p\delta_{ij} \tag{5}$$

where k is the hardening function for the pore collapse mechanism and h a material parameter defining the ratio of the two axes of the elliptic yield surface. p and q respectively designate the mean stress and the deviator of the stress tensor. As the pore collapse mechanism is physically related to irreversible modification of pore volume, it is assumed that the material hardening for this mechanism depends on the plastic volumetric strain ε^p_c. Therefore, the following plastic hardening law is proposed:

$$k = k_0 e^{a.\varepsilon^p_c} \tag{6}$$

where k_0 and a are respectively the initial pore collapse threshold and a plastic hardening parameter.

According to experimental data from porous chalks, it has been found that a non-associated flow rule should be used for this type of rock for the pore collapse mechanism. In the present model an elliptical flow rule has been chosen in accordance with the form of the yield surface:

$$g_c = h_c^2\, q^2 + p^2 \tag{7}$$

where parameter h_c defines some deviation of the plastic flow from the normal to the yield surface. It makes possible to better describe the path dependency of collapse plastic strains.

Deviatoric Mechanism

During deviatoric loading, the plastic deformation results essentially from sliding and from microrotations of grains: material failure occurs by shearing. From experiment data, the plastic yield function for the matrix shearing is proposed by extending the classical Drucker-Prager criterion:

$$f_d = q(\cos\theta + \frac{\alpha_m}{\sqrt{3}}\sin\theta) - \alpha(p + p_0) = 0 \tag{8}$$

where the effect of Lode angle is included:

$$\theta = \frac{1}{3}\arcsin\left[\frac{3\sqrt{3}}{2}\frac{J_3}{\sqrt{J_2^3}}\right] \tag{9}$$

In order to account for chalk responses in complex loading paths, the yield function of the deviatoric mechanism depends on the three basic stress invariants p, q and J_3 (or Lode angle noted θ). This way to take into account the Lode angle dependency of material behaviour was used by several authors, for instance Papamichos *et al.* (1995). α is the hardening function representing the current value of material friction and p_0 the hydrostatic tensile strength assumed to be constant. The strain-hardening rule of the deviatoric mechanism is described by the evolution of the friction α from its initial value α_0 to its ultimate value α_m. The following equation is proposed:

$$\alpha = \alpha_m - (\alpha_m - \alpha_0)e^{-b\gamma_d} \quad \text{and:} \quad \gamma_d = \sqrt{\frac{2}{3}e_{ij}^d e_{ij}^d} \tag{10}$$

where e_{ij}^d is the deviatoric plastic strain and b a material hardening parameter.

Like most rocks, the plastic flow in deviatoric mechanism is generally non-associated and the following plastic potential is proposed:

$$g_d = q + \beta p \tag{11}$$

where β is the plastic dilatancy coefficient. In order to consider the progressive transition from plastic compressibility to dilatancy in most rocks it is proposed that β decreases with the generalised deviatoric plastic strain as follows:

$$\beta = \beta_0\, e^{-b\gamma_d} \tag{12}$$

where β_0 defines the initial value of β and b (the same as that in Eq. (10)) is a material hardening parameter.

Determination of the Model Parameters

The parameters of this model may be determined from conventional laboratory tests (triaxial and hydrostatic tests). The method used for their determination will be given below.

The Pore Collapse Mechanism Parameters

The plastic yield function and the plastic potential concerning the pore collapse mechanism involve four parameters called h, k_0, a and h_c. The value of h can be determined by drawing the elliptic surface from initial yield stresses obtained from hydrostatic and triaxial tests with "high" confining pressure *(Fig. 1a)*. k_0 can be directly evaluated from the hydrostatic test: its value corresponds to the mean pressure after which irreversible deformations occur in a material during this test. a is obtained from a hydrostatic compression test, it represents the slope of the curve plotting the plastic volume deformation as a function of the logarithm of the mean stress divided by the pore collapse threshold ratio *(Fig. 1b)*:

$$\ln\frac{\sigma_m}{k_0} = a\varepsilon_c^p \tag{13}$$

Finally, the parameter h_c involved in the plastic potential can be identified by plotting the increment of plastic strains at a given stress state during a triaxial test with high confining pressure where only the collapse mechanism is active (Homand, 2000).

The Deviatoric Mechanism Parameters

The plastic yield function and the plastic potential concerning the deviatoric mechanism involve five parameters called p_0, α_m, α_0, β_0 and b. The values of p_0, α_m and α_0 can be determined from a minimum of three triaxial tests at low confining pressure conducted until failure of sample. The plot in the p-q plane of the initial yield stresses and of the peak stresses provides two straight lines with respective slopes of α_0^* and α_m^*. Hydrostatic tensile strength p_0^* is given by the intersection of these two straight lines with the p (mean stress) axis *(Fig. 1c)*. For triaxial compression, by putting the value of the Lode angle $\theta = -\pi/6$ respectively into the initial yield condition ($\alpha = \alpha_0$) and failure condition ($\alpha = \alpha_m$) in Equation (8), we obtain easily the values of α_0 and α_m from α_0^* and α_m^* as well as $p_0 = p_0^*$.

To determine the hardening parameter b, we use the plastic loading phase of a triaxial test. As the parameters p_0, α_m and α_0 are previously determined, the use of the consistence conditions $f_d = 0$ allows to calculate the current value of friction coefficient α:

$$\alpha = \frac{q\left(\frac{\sqrt{3}}{2} - \frac{\alpha_m}{2\sqrt{3}}\right)}{p + p_0} \tag{14}$$

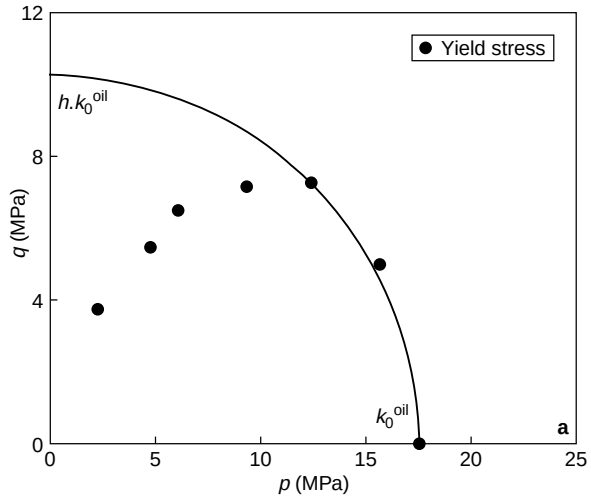

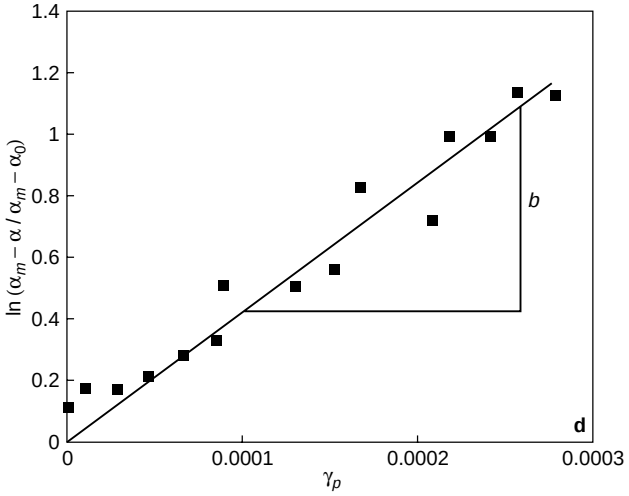

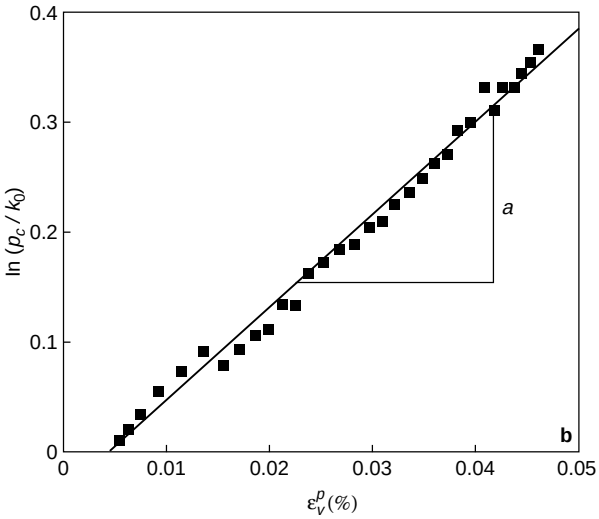

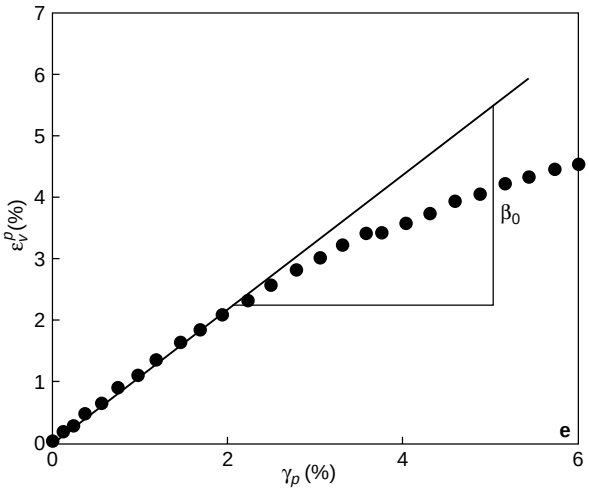

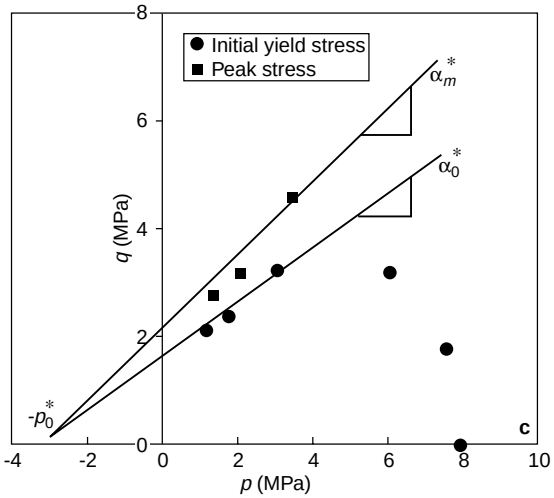

Figure 1

Determination of the model parameters.
(a) h; (b) a; (c) p_0, α_m, α_0; (d) b; (e) b_0.

The strain hardening function *(Eq. (10))* can be rewritten in logarithmic form:

$$\ln\left(\frac{\alpha_m - \alpha}{\alpha_m - \alpha_0}\right) = -b\gamma_d \qquad (15)$$

As the generalised deviatoric plastic strain γ_d can be calculated at each stress state during plastic phase, the plot of Equation (15) allows to determine b from a linear regression *(Fig. 1d)*. However, as can be expected from the different shapes obtained for the different triaxial tests, this parameter may be sensible to the confining pressure. The solution used

for this study is to consider an average of the different values obtained for different confining pressures.

β_0 is obtained by plotting the plastic volumetric strain ε_v^d as a function of the plastic deviatoric strain γ_d: β_0 is the initial slope of this curve. This parameter actually governs the partition of the deformation tensor into its volumetric and deviatoric parts:

$$\begin{bmatrix} d\varepsilon_v^d \\ d\gamma_d \end{bmatrix} = d\lambda \begin{bmatrix} \partial g_d / \partial p \\ \partial g_d / \partial q \end{bmatrix} = d\lambda \begin{bmatrix} \beta \\ 1 \end{bmatrix} \tag{16}$$

then: $d\varepsilon_v^d/d\gamma_d = \beta$ with $\beta = \beta_0 e^{-b\gamma_d}$ and: $d\varepsilon_v^d/d\gamma_d|_{\gamma_d=0} = \beta_0$ at the start of the plastic loading *(Fig. 1e)*.

For the chalk studied here, two sets of model parameters corresponding to the two different saturating fluids are determined for the two material states of chalk *(Table 1)*, by using the procedure presented here above.

TABLE 1

Values of model parameters for two material states of chalk

Parameters	Oil saturated state	Water saturated state
E	4200 MPa	3700 MPa
v	0.2	0.2
h	1.9	1.5
k_0	17.5 MPa	7.9 MPa
a	15	15
p_0	3 MPa	1.5 MPa
α_0	0.48	0.48
α_m	0.68	0.65
b	5000	5000
β_0	0.8	0.8
h_c	1.2	1.2

Plastic Flow Rules

The flow rules establish the direction of the plastic strain increments by taking the gradient to the plastic potential. Therefore, for the pore collapse and deviatoric mechanism the plastic strain increments are respectively:

$$d\varepsilon_{ij}^c = d\lambda_c \frac{\partial g_c}{\partial \sigma_{ij}} \quad \text{and:} \quad d\varepsilon_{ij}^d = d\lambda_d \frac{\partial g_d}{\partial \sigma_{ij}} \tag{17}$$

In the case of multisurface model, the plastic multipliers are determined by solving a linear system expressing the consistency conditions for each surface (Simo *et al.*, 1988; Pramono and Williams, 1989):

$$\begin{cases} \dfrac{\partial f_c}{\partial \sigma} d\sigma + \dfrac{\partial f_c}{\partial \varepsilon_v^p} d\varepsilon_v^p = 0 \\ \dfrac{\partial f_d}{\partial \sigma} d\sigma + \dfrac{\partial f_d}{\partial \gamma_d} d\gamma_d = 0 \end{cases} \tag{18}$$

Effect of Saturating Fluid on Chalk Behaviour

The laboratory results presented in the first part of the study (Homand and Shao, 2000) have clearly shown that the mechanical behaviour of chalk is strongly sensitive to the nature of saturating fluid. In this study, the validation of the new approach for numerical modelling of this phenomenon proposed by Homand *et al.* (1998) is made possible by using the laboratory investigations mentioned above. This approach assumed that there are two chalk material states, dried or oil saturated and water saturated, superposed on the same material point. When the water saturation is less than the critical value S_w^c, the "oil" chalk behaviour is active. On the other hand, the "water" chalk should be considered when the water saturation is higher than the critical value. Moreover, the two chalk materials can be described by the same formal constitutive model, but associated with two distinct sets of material parameters. Consequently, water injection causes a jump of yield surfaces from the "oil state" to "water state" and the plastic equilibrium is disturbed. The way to re-establish this plastic equilibrium is to produce an instantaneous plastic deformation. Therefore, the water induced plastic strains can be expressed by:

$$d\varepsilon_{ij} = d\varepsilon_{ij}^e + d\varepsilon_{ij}^p + \Delta\lambda_w \frac{\partial g_w}{\partial \sigma_{ij}} \tag{19}$$

with:

$$\begin{aligned} &\Delta\lambda_w > 0 \quad \text{if: } S_w^t < S_w^c \quad \text{and: } S_w^{t+\Delta t} > S_w^c \\ &\Delta\lambda_w = 0 \quad \text{else} \end{aligned} \tag{20}$$

In the previous equations, S_w^c is the critical water saturation degree. g_w is a potential which determines the direction of water induced plastic strain and is determined from laboratory testing. In this paper, a linear potential is proposed:

$$g_w = q + \beta_w p \tag{21}$$

The value of the plastic multiplier $\Delta\lambda_w$ is determined from the differences in material parameters between the two chalk material states. In a simplified scheme, we assume that the water flooding effect is represented by a jump of the elliptic yield surface only through a reduction of the initial pore collapse threshold k_0. Therefore, the plastic multiplier $\Delta\lambda_w$ can be explicitly determined from the plastic equilibrium condition between two material states (under constant stresses) as follows:

$$\Delta\lambda_w = \frac{1}{\beta_w} \frac{1}{a} \ln\left(\frac{k_0^{\text{oil}}}{k_0^{\text{water}}} \right) \tag{22}$$

where k_0^{oil} and k_0^{water} are respectively the pore collapse threshold for "oil" and "water" states of chalk.

Simulation of Laboratory Tests

In this section, numerical simulations of some representative laboratory tests are performed by using the proposed constitutive model. Comparisons between numerical results and test data make it possible to check the validity of the model.

In Figure 2, the simulations of two hydrostatic compression tests respectively performed on "oil saturated" and "water saturated" samples are shown. The good correlation between numerical and experimental data indicates that the weakening effect of water on plastic pore collapse of chalk is well described. In Figures 3 and 4, two series of triaxial compression tests with different confining pressures, respectively in water and oil saturated conditions, are simulated by using the proposed elastoplastic model and the sets of parameters given in Table 1. There is also an overall good agreement between numerical and experimental results. In Figure 5, three lateral extension tests are simulated. In this test, the sample is first submitted to a hydrostatic stress up to a prescribed value (noted P_{ci}). Then the lateral stress is decreased while the axial stress is kept constant. Axial and lateral strains are obtained as functions of the deviatoric stress. This kind of loading path is particularly interesting in rock mechanics field and used as a fundamental test to check the validity of constitutive models. Indeed, such a loading path is relevant to represent stress disturbances around a tunnel due to excavation. The comparison in Figure 5 shows a good correlation. In Figure 6, two proportional compression tests are simulated. In this test, the sample is submitted to a deviatoric stress state with a constant ratio between the lateral and the axial stresses. A good correlation is obtained both for high and low stress ratios. As a conclusion, the proposed model seems to be valid to describe the basic mechanical behaviour of porous rocks, both in "oil" and "water" saturation conditions.

In order to check the capacity of the proposed constitutive model to predict plastic deformation of chalk due to water flooding, the model is applied to simulate the water injection tests presented in the first part of this study. The simulations have been carried out by using a Finite Element Method code. However these tests have been performed on samples coming from a different block of chalk than those used for all the previous tests: pore collapse is higher for this new set of samples. Different model parameters should be determined. By putting the main aim here on the modelling of the water induced strain, some simplifications have been proposed. Only two representative plastic parameters depend on the saturating fluids (the pore collapse threshold k_0 and the tensile strength p_0), and the others have been considered as independent of the saturating fluid and an average value has been chosen for each one. The sets of parameters used for the following simulations are summarised in Table 2.

Numerical results in different water injection conditions are presented and compared with experimental data. In Figures 7 and 8, we present the evolution of axial and lateral strains at three height levels of sample (level locations are presented in the experimental study, see Homand and Shao (2000)). There is a good correlation between numerical and experimental results for the axial strain. Quantitative scatters are observed on the lateral strain. In Figures 9 and 10, we present the evolution of the axial and lateral strains at the middle point of sample, obtained in the different water injection tests under constant stress conditions listed in Table 3.

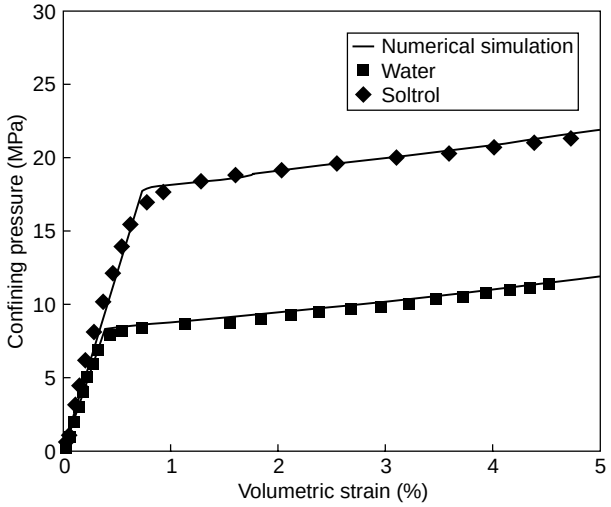

Figure 2

Simulations of hydrostatic tests for different saturating fluids (water and soltrol).

TABLE 2

Values of model parameters for two material states of chalk used for simulation of water injection tests

Parameters	Oil saturated state	Water saturated state
E	4200 MPa	3700 MPa
ν	0.2	0.2
h	1.7	1.7
k_0	21 MPa	12 MPa
a	15	15
p_0	3 MPa	1.5 MPa
α_0	0.48	0.48
α_m	0.67	0.67
b	5000	5000
β_0	0.8	0.8
h_c	1.2	1.2
β_w	2	2

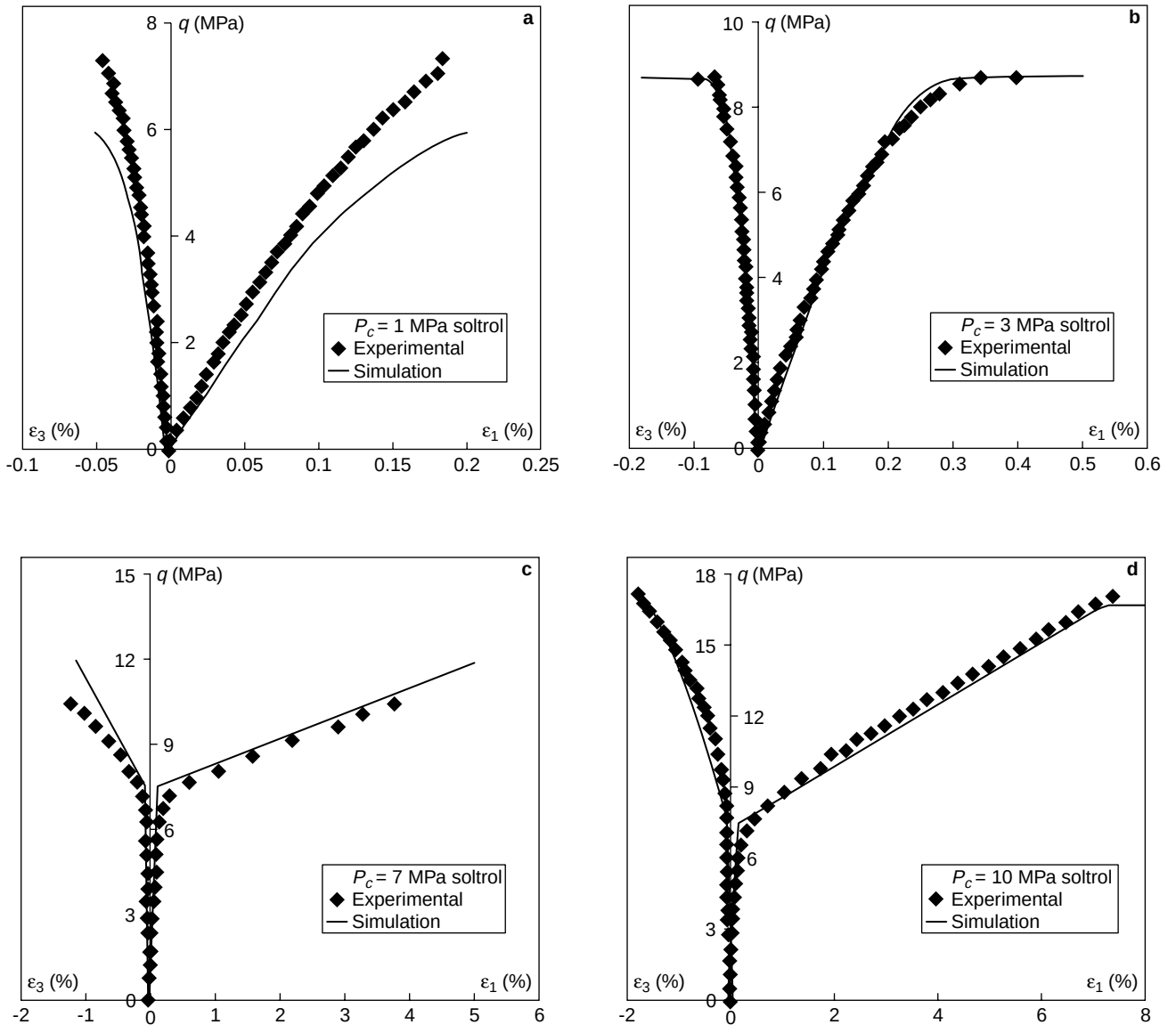

Figure 3

Simulation of triaxial tests for different confining pressures (soltrol saturated).
(a) P_c = 1 MPa; (b) P_c = 3 MPa; (c) P_c = 7 MPa; (d) P_c = 10 MPa.

TABLE 3

Applied stress states for water injection tests

Test designation	Confining pressure (MPa)	Deviator (MPa)
SLIX1INJ	17	9
SLIX2INJ	14	4.5
SLIX3INJ	17	3.5
SLIX4INJ	25	0
SLIX5INJ	20	3.1

Once again, a good correlation is obtained. In each case, the qualitative response of chalk, for instance, the instantaneous and local character of the induced plastic deformation during the passage of water front, is fully reproduced. From a quantitative point of view, the magnitude of induced strains is also correctly recovered in most cases.

We should note that the induced plastic strains are not uniform in sample due to water flooding. The values measured by gauges represent an average strain in the small zone around the gauge location while the numerical values

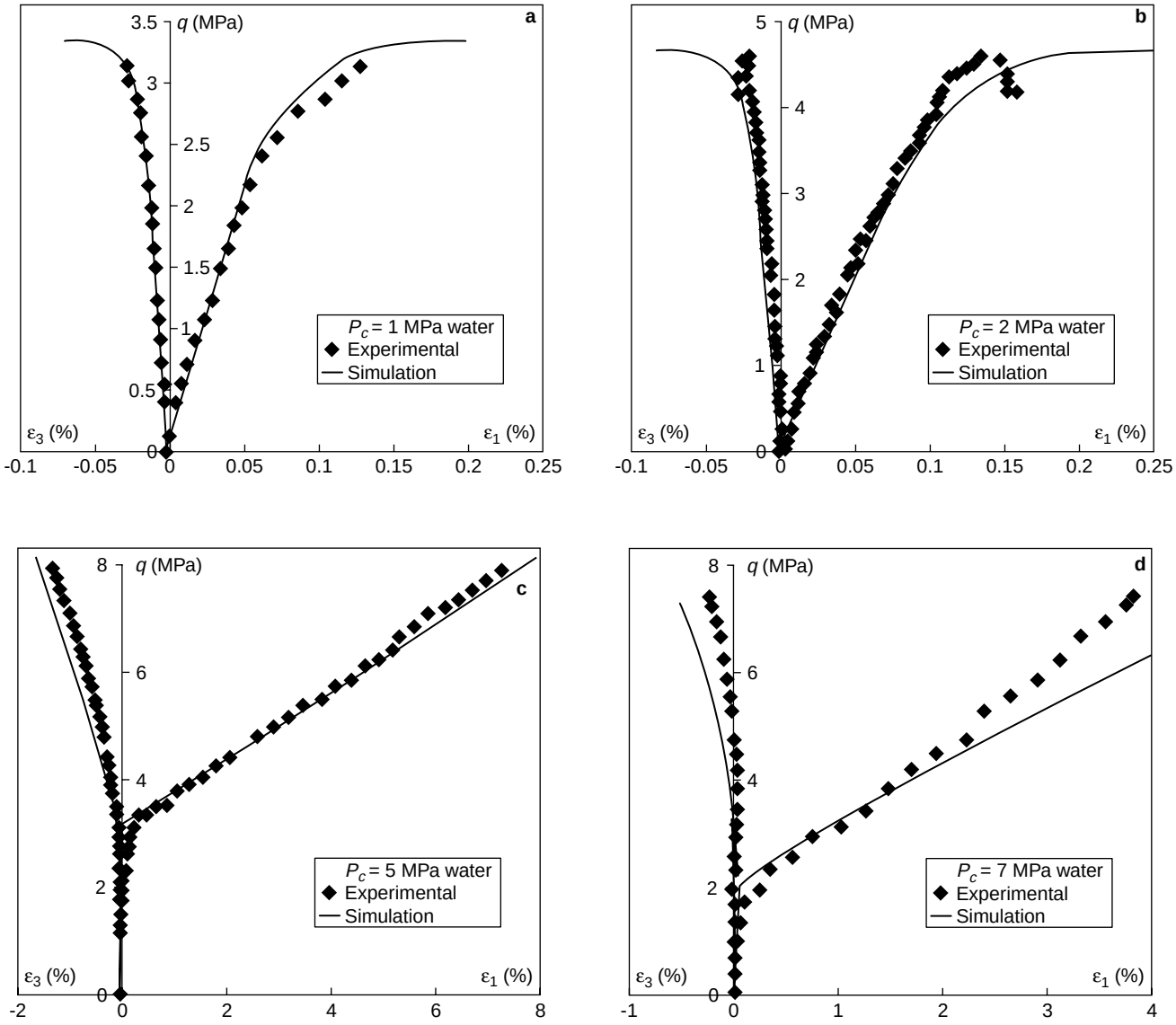

Figure 4

Simulation of triaxial tests for different confining pressures (water saturated).
(a) P_c = 1 MPa, (b) P_c = 2 MPa, (c) P_c = 5 MPa; (d) P_c = 7 MPa.

are obtained at the closest Gauss points to gauge centres. In addition, a special surface treatment was necessary to glue strain gauges on porous chalk. Errors are certainly included in experimental data, in particular when strains are small like the case of lateral strain. Therefore, the quality of the numerical simulations seems to be satisfactory. Moreover, a linear water plastic potential g_w has been used for this study and it seems that a more elaborated potential (elliptic potential for example) should be used.

CONCLUSIONS

In the second part of this study, an elastoplastic model with two yield mechanisms has been proposed on the basis of test data. The capacity of the model to describe the basic behaviour of chalk has been tested for some specific loading paths. Further validation tests are still necessary to get an overall appreciation of the performance of the model.

A new way has been developed to determine the water flooding induced plastic deformation. It is based on the idea

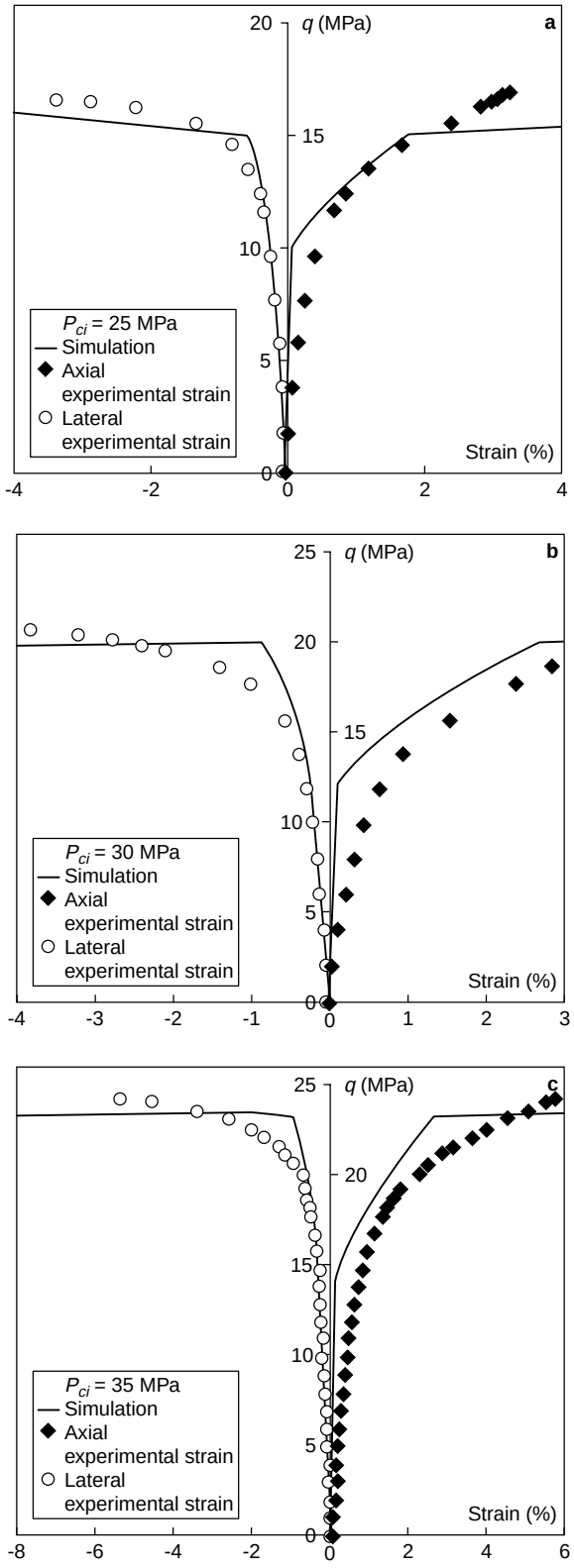

Figure 5

Simulation of lateral extension tests with different initial confining pressures (soltrol saturated).
(a) P_{ci} = 25 MPa; (b) P_{ci} = 30 MPa; (c) P_{ci} = 35 MPa.

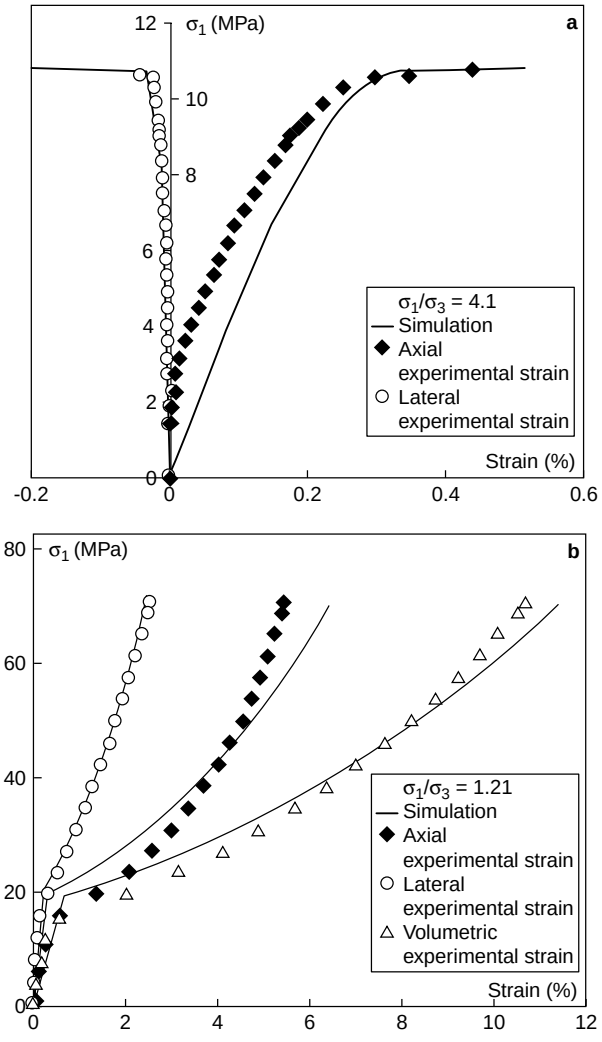

Figure 6

Simulation of proportional loading tests with different stress ratios (oil saturated).
(a) σ_1/σ_3 = 4.1.
(b) σ_1/σ_3 = 1.21.

that the chalk presents a behaviour jump between two material states when it is flooded by water. The validity of the model is checked by simulating water injection tests under different stress conditions. A good quality of numerical predictions is obtained.

The proposed model will be applied to study oil reservoir compaction during water injection process.

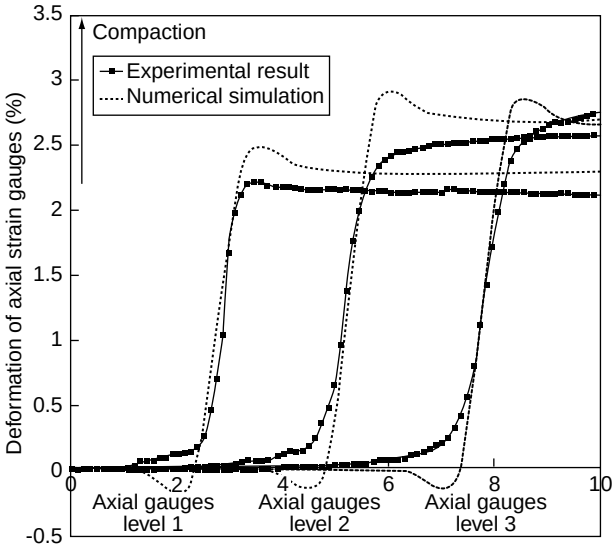

Figure 7

Simulation of the axial displacement induced by water injection in a soltrol saturated chalk sample under constant stress conditions.
P_c = 17 MPa, q = 3.5 MPa.

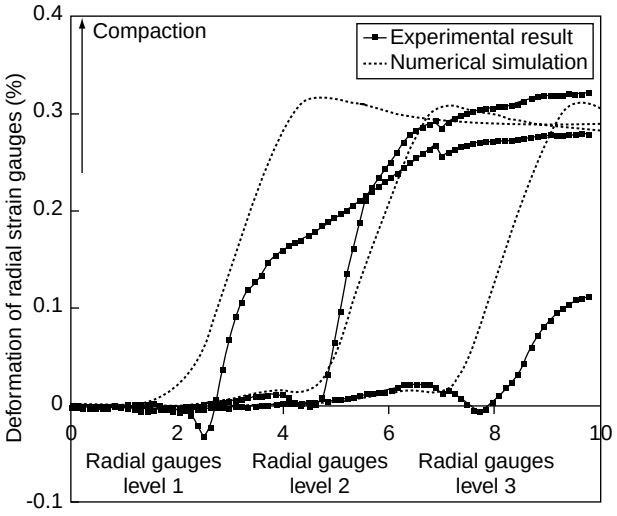

Figure 8

Simulation of the radial deformations induced by water injection in a soltrol saturated chalk sample under constant stress conditions.
P_c = 17 MPa, q = 3.5 MPa.

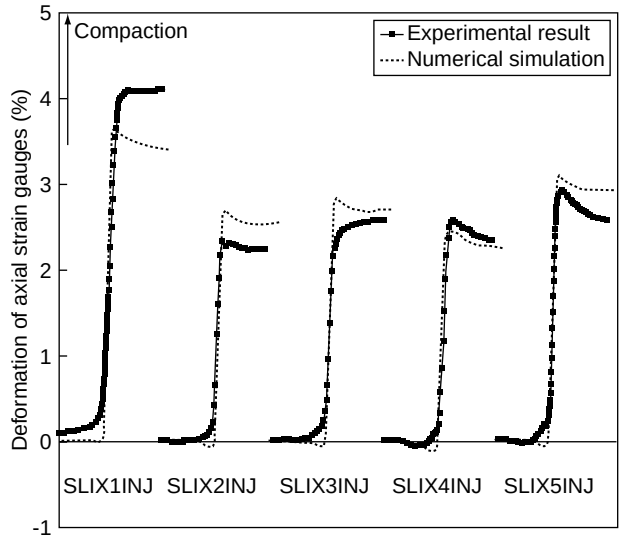

Figure 9

Simulation of the axial deformations induced by water injection in a soltrol saturated chalk sample under various constant stress conditions (gauges located on the middle of the sample).

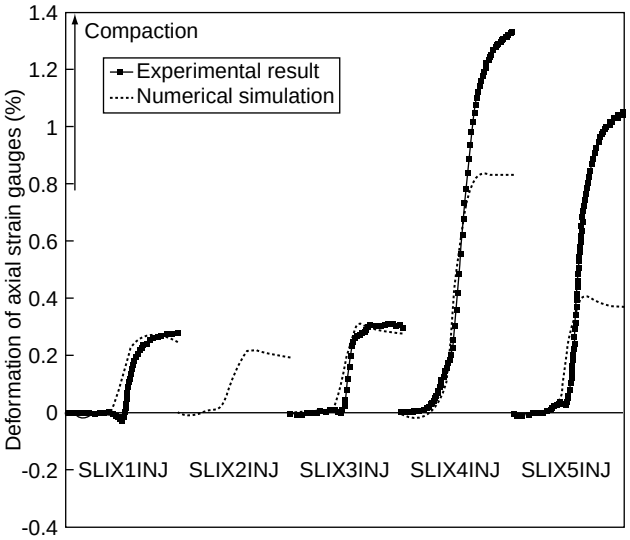

Figure 10

Simulation of the radial deformations induced by water injection in a soltrol saturated chalk sample under various constant stress conditions (gauges located on the middle of the sample).

REFERENCES

Drucker, D.C., Gibson, R.E. and Henkel, D.J. (1957) Soil Mechanics and Work Hardening Theories of Plasticity. *Trans. ASCE*, 122, 338-346.

Halleux, L., Detiege, C., Poot, B., Schroeder, C., Monjoie, A., Debande, G. and Da Silva, F. (1990) Mechanical Behaviour of Chalks. *Proc. of the 2nd North Sea Chalk Symposium*, Copenhagen.

Homand, S. (2000) Comportement mécanique d'une craie très poreuse avec prise en compte de l'effet de l'eau : de l'expérience à la simulation (Mechanical Behaviour of a Porous Chalk and Water Effects: Experimental Investigation and Numerical Modelling). *PhD Thesis*, University of Lille.

Homand, S. and Shao, J.F. (2000) Mechanical Behaviour of a Porous Chalk and Water/Chalk Interaction, Part I: Experimental Study. *Oil & Gas Science and Technology*, **55**, 6, 591-598.

Homand, S., Shao, J.F. and Schroeder, C. (1998) Plastic Modelling of Compressible Porous Chalk and Effect of Water Injection. *Proc.of Eurock '98—Rock Mechanics in Petroleum Engineering*, Trondheim, *SPE/ISRM 47585*, 495-504.

Monjoie, A., Schroeder, C. and Da Silva, F. (1995) Mechanical Behaviour of Chalks. *Proc. of the 3rd North Sea Chalk Symposium*, Stavanger.

Papamichos, E., Brignoli, M. and Santarelli, F.J. (1997) An Experimental and Theoretical Study of a Partially-Saturated Collapsible Rock, in *Mechanics of Cohesive-Frictional Materials*, Vol. 2, 251-278.

Piau, J.M. and Maury, V. (1994) Mechanical Effects of Water Injection on Chalk Reservoirs. *Proc. of Eurock '94—Rock Mechanics in Petroleum Engineering*, Delft, Balkema, Rotterdam, *SPE/ISRM 28133*, 837-843.

Piau, J.M. and Maury, V. (1995) Basic Mechanical Modelisation of Chalk/Water Interaction. *Unsaturated Soils*, 215-244.

Piau, J.M., Bois, A.P., Atahan, C., Maury, V. and Hallé, G. (1998) Water/Chalk Interaction: Part I. Comprehensive Evaluation of Strain and Stress Jumps at the Waterfront. *Proc. of Eurock '98—Rock Mechanics in Petroleum Engineering*, Trondheim, 419-428.

Pramono, E. and Willam, K. (1989) Implicit Integration of Composite Yield Surfaces with Corners. *Eng. Comput.*, **6**, 186-197.

Schroeder, C. (1995) Le Pore Collapse : aspect particulier de l'interaction fluide-squelette dans les craies ? *Proc. of the Colloque international du Groupement belge de mécanique des roches*, Brussels.

Shao, J.F. and Henry, J.P. (1991) Development of an Elastoplastic Model for Porous Rock. *International Journal of Plasticity*, **6**, 1, 1-13.

Shao, J.F., Dahou, A. and Bederiat, M. (1995) Experimental and Numerical Investigations on Transient Creep of Porous Chalk. *Mechanics of Materials*, 21, 147-158.

Simo, J.C., Kennedy, J.G. and Govindjee, S. (1988) Non-Smooth Multisurface Plasticity and Viscoplasticity. Loading/Unloading Conditions and Numerical Algorithms. *International Journal for Numerical Methods in Engineering*, **26**, 2161-2185.

Final manuscript received in October 2000